arXiv:physics/0311012v1 [physics.bio-ph] 4 Nov 2003

Transverse fluctuations of grafted polymers

G. Lattanzi[1] T. Munk[2] and E. Frey[1,2]

[1] *Abteilung Theorie, Hahn-Meitner-Institut, Glienicker Strasse 100, 14109 Berlin, Germany*

[2] *Fachbereich Physik, Freie Universität Berlin, Arnimallee 14, 14195 Berlin, Germany*

(Dated: October 26, 2021)

Abstract

We study the statistical mechanics of grafted polymers of arbitrary stiffness in a two-dimensional embedding space with Monte Carlo simulations. The probability distribution function of the free end is found to be highly anisotropic and non-Gaussian for typical semiflexible polymers. The reduced distribution in the transverse direction, a Gaussian in the stiff and flexible limits, shows a double peak structure at intermediate stiffnesses. We also explore the response to a transverse force applied at the polymer free end. We identify F-Actin as an ideal benchmark for the effects discussed.

PACS numbers: 87.15.Ya, 87.15.La, 87.16.Ka, 36.20.Ey

Healthy cells require an efficient and complex transport network to carry out the overwhelming number of tasks that are needed to accomplish their function. This network, also known as the *cytoskeleton*, is formed primarily by *filaments* (actin filaments, microtubules and intermediate filaments), linked together by a large collection of accessory proteins [1]. A complete description of the structural and mechanical properties of these filaments is therefore essential in order to unveil the mechanical properties of the entire cell. Advances in the field have been significantly promoted by a unique set of optical and mechanical techniques which allow to visualize and manipulate single cytoskeletal filaments [2, 3, 4] and DNA [5]. Fluorescence videomicroscopy [6] and nano-manipulation [7] can be conveniently used to obtain quantities as the distribution function of the end-to-end distance [6] or the mechanical response to an external force in great detail and at the single molecule level. These quantities are amenable to a direct comparison with theoretical models.

The main material parameter in the description of a polymer filament is its persistence length, ℓ_p. It is defined as the typical length over which correlations of the tangent vectors of the filament contour decay. Polymers are considered to be flexible when their persistence length is small compared to their total length L, or $t := L/\ell_p \gtrsim 10$. In this limit, they can be well described by the minimal model of the Gaussian Chain [8]. Polymers of biological importance, e.g. F-actin, are often semiflexible, meaning that their persistence length is comparable to their total length. While flexible polymers are dominated by entropic effects, the statistical mechanics of semiflexible polymers is strongly affected by their bending energy and the close vicinity of the classical Euler instability for buckling a rigid beam [9].

The distribution function $P(\vec{R})$ of the end-to-end vector $\vec{R}$, a simple Gaussian for a flexible polymer, is peaked towards full stretching and is completely non-Gaussian [10]. The mechanical response of a semiflexible polymer is highly anisotropic, depending on the direction in which the force is applied [11]. These findings result in bulk properties of solutions and networks that are completely different from the isotropic elasticity of flexible polymer solutions [12, 13]. In addition, the inextensibility constraint becomes crucial in determining the approach to full stretching upon the application of a force f, as reported by Marko and Siggia [5] for double–stranded DNA.

Here we investigate the mechanical and statistical properties of a single chain grafted at one end, a problem of direct relevance for force generation in cellular systems. The other end is either free, or subject to a constant transverse force, whose magnitude extends

into the non–linear regime. We restrict ourselves to a two–dimensional embedding space, since in most experiments, fluctuations in one direction are severely restricted, or cannot be observed. The generalization to a three–dimensional space is straightforward and will be reported elsewhere [14].

We refer to the Wormlike Chain Model (WLC) introduced by Kratky and Porod [15]. In this framework, a polymer conformation is represented by a succession of N segments $\vec{t}_i$, whose direction is tangent to the polymer contour at the ith segment. Since the polymer is assumed to be inextensible, all segments $\vec{t}_i$ have a prescribed length $a = L/N$. The Hamiltonian is given by:

$$\mathcal{H} = -\varepsilon \sum_{i=1}^{N-1} \vec{t}_i \cdot \vec{t}_{i+1} - \sum_{i=1}^{N} \vec{f} \cdot \vec{t}_i \,, \tag{1}$$

where ε is the energy associated to each bond and $\vec{f}$ is a force eventually applied to the second end. It is also possible to define a continuum limit for $a \to 0$, $N \to \infty$, with $Na = L$ and $\epsilon = \varepsilon a^2/N$ held fixed. The Hamiltonian in Eq. 1 is then equivalent to the following functional [16, 17]:

$$\mathcal{H}_f = \frac{\kappa}{2} \int_0^L ds \left(\frac{\partial \vec{t}(s)}{\partial s} \right)^2 - \vec{f} \cdot \int_0^L ds \; \vec{t}(s) \,, \tag{2}$$

where $\kappa = \epsilon L$ and $\vec{t}(s)$ is the tangent vector of the space curve $\vec{r}(s)$ parametrized in terms of the arc length s. The inextensibility of the filament is imposed by the local constraint $\left|\vec{t}(s)\right| = 1$. The continuous version of the wormlike chain has been successfully used to obtain various statistical quantities, as the tangent-tangent correlation function or moments of the end-to-end distance distribution [16, 18]. It has been recently used to obtain the radial distribution function [10], and force-extension relations [5, 11, 19].

We have developed a Monte Carlo simulation to investigate the behavior of a semiflexible polymer in the proximity of the limit $t \to 1$. The rationale behind this choice is the search for clear hallmarks of the onset of the "semiflexible" nature of a filament. In this intermediate limit, analytical results are difficult to obtain: typical approximation schemes that build on either Gaussian chains or rigid rods are outside their validity range; hence, computer simulations become crucial. The first end of the filament is assumed to be clamped, i.e. the orientation of its tangent vector is held fixed along a direction, named the x-axis. The second end is left free to assume any possible orientation. The initial configuration has been randomly chosen in the proximity of the full stretching condition, thus ensuring a fast convergence to equilibrium. A new configuration is generated by changing the orientation of

one segment and accepted according to the standard Metropolis algorithm and the discrete Hamiltonian, Eq. 1. Effects resulting from self–avoidance are not considered, but we notice that configurations where the chain folds back onto itself are strongly energetically suppressed for sufficiently stiff polymers. Results ceased to depend on the number of segments for $N = 50$. On the order of 10^6 Monte Carlo steps per segment were performed, and results were averaged over different runs, obtaining a perfect agreement between measured expectation values of the end-to-end distance $\langle R^2 \rangle$ and $\langle R^4 \rangle$ with known exact expressions. The radial distribution function was calculated and coincided with the analytic results in [10] within the accuracy thereby reported.

Here we are interested in the probability distribution function $P(x, y)$ of the free end in the plane determined by the direction of the clamped end (x-axis) and the transverse one (y-axis). This quantity is directly accessible to experiments allowing for a quantitative comparison with our predictions. We will also consider the reduced distribution functions $P(x)$ and $P(y)$, obtained by integrating $P(x, y)$ over the variables y and x, respectively.

It is important to notice that when both ends are free, the radial distribution function is rotationally invariant and is therefore only a function of the distance R between the ends. Clamping one end breaks rotational symmetry and leads to distinctly different longitudinal and transverse distribution functions, $P(x)$ and $P(y)$. Nonetheless, the broken rotational symmetry does not affect the total energy of the configuration. This implies, and is in fact confirmed by our simulations (data not shown), that the longitudinal distribution function $P(x)$ coincides with the radial distribution function $P(R)$ of the end-to-end distance, apart from a constant normalization factor. The characteristic feature of this function is a crossover from a universal Gaussian shape centered at the origin with a characteristic width determined by the radius of gyration, to yet another universal shape [10], whose peak is shifted towards full stretching and whose width is determined by a new longitudinal length scale $L_\parallel \propto L^2/\ell_p$.

This has to be contrasted with the transverse distribution function. Not surprisingly, given the intrinsic isotropy of flexible polymers, the distribution $P(y)$ is a Gaussian and identical to $P(x)$ for high values of t. In the stiff limit, $P(y)$, at variance with $P(x)$, is again a Gaussian centered at $y = 0$, whose width is now given by a new transverse length scale $L_\perp = \sqrt{2L^3/3\ell_p}$ [20, 21]. Surprisingly, at intermediate values the probability distribution function is not a smooth interpolation between these two Gaussian limits but shows interesting and qualitatively new features. As t approaches the value 1 from above

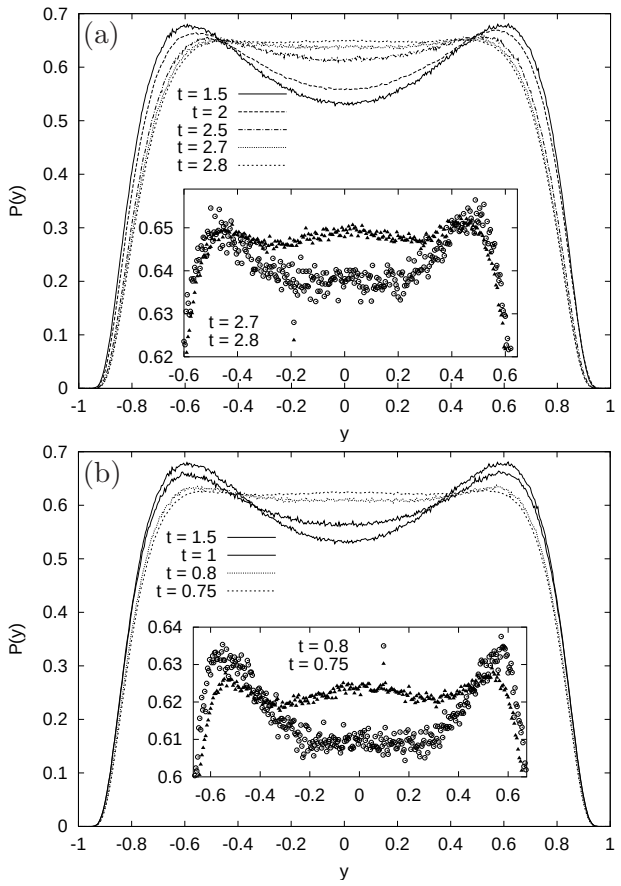


FIG. 1: Distribution function for the projection of the free end along the transverse direction, $P(y)$, obtained by Monte Carlo simulations. Lengths are measured in units of L. Errors are comparable to the point size in the insets. (a) Appearance of double peaks for $t \lesssim 2.5$. (b) Re-entrance from the double peaks to a flat distribution in the stiff limit $t \lesssim 0.75$. Insets show details of the crossover regions.

(flexible side), the Gaussian peak is first smeared out into an intrinsically non-Gaussian flat distribution (see Fig. 1a). At $t = 2.8$ (see inset), the distribution contains three local maxima, but as t is decreased, the central peak at $y = 0$ loses weight to the two symmetric peaks off the x axis. The double-peak structure is most pronounced around $t \approx 1.5$, i.e. $L \approx 1.5\ell_p$.

As the stiffness is increased, $P(y)$ recovers its flat structure, as shown in Fig. 1b. Notice also (inset of Fig. 1b) that at $t = 0.75$ the two peaks start to compete with a growing peak centered at $y = 0$, such that one finds a triple maxima shape again. Although intrinsically non–Gaussian, this central peak will eventually tend to a Gaussian distribution in the stiff limit. The re-entrance from the double peak structure to a flat distribution is a genuine

hallmark of semiflexibility. This effect cannot be explained by analytical calculations using a harmonic (or weakly bending rod) approximation, whose prediction for $P(y)$ would be a Gaussian centered at 0 [20]. Higher order cumulant expansions about a Gaussian distribution have also failed to provide a fast convergence to our $P(y)$. An entirely analytical solution can be provided by the eigenfunction approach described in [22] for persistent random walks, although the connection to our probability distributions would only be numerical.

Finally, let us emphasize that the double-peak structure of $P(y)$ does not indicate a bistability in the constant force ensemble. As shown below, linear response theory leads to positive force constants in this regime. What actually happens under the application of an external force is that the distribution function becomes asymmetric and weight is shifted from one peak to the other. In an experimental setting with a fixed transverse distance y and a correspondingly adjusting force, one would probe $P(y)$ directly and be able to observe a kind of "bistability".

Further insight can be gained by the inspection of the joint distribution function $P(x, y)$, represented with density plots in Fig. 2. In the stiff limit, $P(x, y)$ should be confined to the

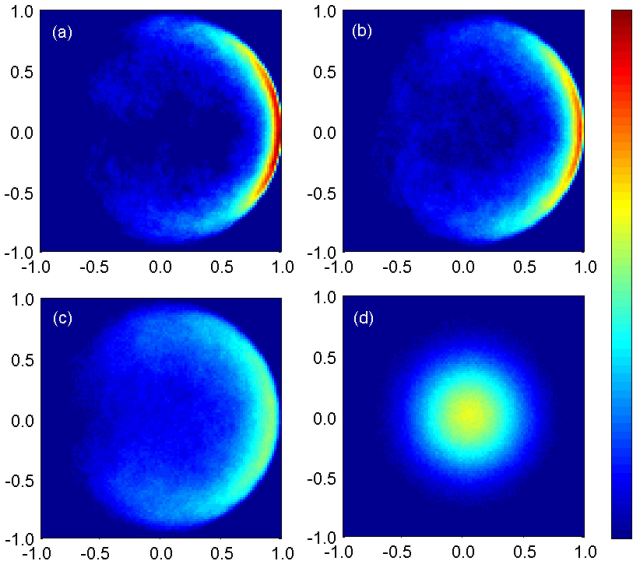


FIG. 2: Density plots obtained by Monte Carlo simulations: dense regions are colored in red, scarcely populated in blue on a color scale appropriately chosen to enhance the contrast. (a) $t = 2/3$; (b) $t = 1$; (c) $t = 2$; (d) $t = 20$.

classical contour obtained by applying the elasticity equations to a rigid rod. This contour can be approximated by a parabola in the proximity of full stretching and is obtained through

elliptic functions for any deformation [9]. In Fig. 2a the classical contour coincides with the ridge of the probability distribution function. As we relax the stiffness, thermal fluctuations will make the tip of the filament explore the configuration space in the vicinity of the classical contour. Roughly speaking, transverse (bending) fluctuations enhance fluctuations along the classical contour and shift weight from the center to the upper and lower wings in Fig. 2a–b. In contrast, longitudinal fluctuations widen the distribution function perpendicular to the classical contour. Since for a semiflexible polymer, the corresponding lengths $L_{\parallel}$ and $L_{\perp}$ scale differently (transverse fluctuations are much "softer" than longitudinal ones), upon lowering the stiffness $P(x, y)$ gains more weight in the wings rather than in the center. It is precisely this effect that gives rise to the double peak distribution, when $P(x, y)$ is projected in the transverse direction (see Fig. 2b). Eventually, in the flexible limit, where transverse and longitudinal fluctuations become comparable, $P(x, y)$ is spread so as to cover almost all the available space (Fig. 2c), before the isotropic Gaussian distribution is recovered (Fig. 2d).

We have also explored the transverse response of semiflexible polymers by applying a constant force f in the transverse direction. The effect of a small applied force on the average end-to-end distance (or force extension relation) has been studied within linear-response in [11]. In this work, we will consider the effect of an external transverse force of arbitrary magnitude on the average position $\langle x \rangle_f$ and $\langle y \rangle_f$ of the free end.

In general, we expect $\langle y \rangle_f$ to have the same parity of the applied force, and hence to be odd, while $\langle x \rangle_f$ should not depend on the sign of the force and hence should be even. In the continuum limit, it is possible to write down the exact expressions for $\langle x \rangle_f$ and $\langle y \rangle_f$ and to show that the expected parities hold on very general grounds and that the response of the longitudinal extension to a transverse force is intrinsically nonlinear in the small force regime. Monte Carlo simulations confirm these predictions, as shown in Fig. 3. The response in the direction of the clamped end is even in f and it can be approximated by a parabola centered on the $f = 0$ axis. The response in the transverse direction is odd in f and shows the same re-entrance phenomenon reported in [11] for the linear response coefficient.

Note that while in the case of a longitudinal force, the approach towards full stretching (or saturation) can be calculated within the weakly bending rod approximation, this is no longer true for transverse forces. The position of the free end can be calculated from classical elasticity theory [9] and expressed by means of elliptic functions. Only in the high force regime or in the stiff limit, when fluctuations become unimportant, results from our

simulations coincide with classical elasticity theory.

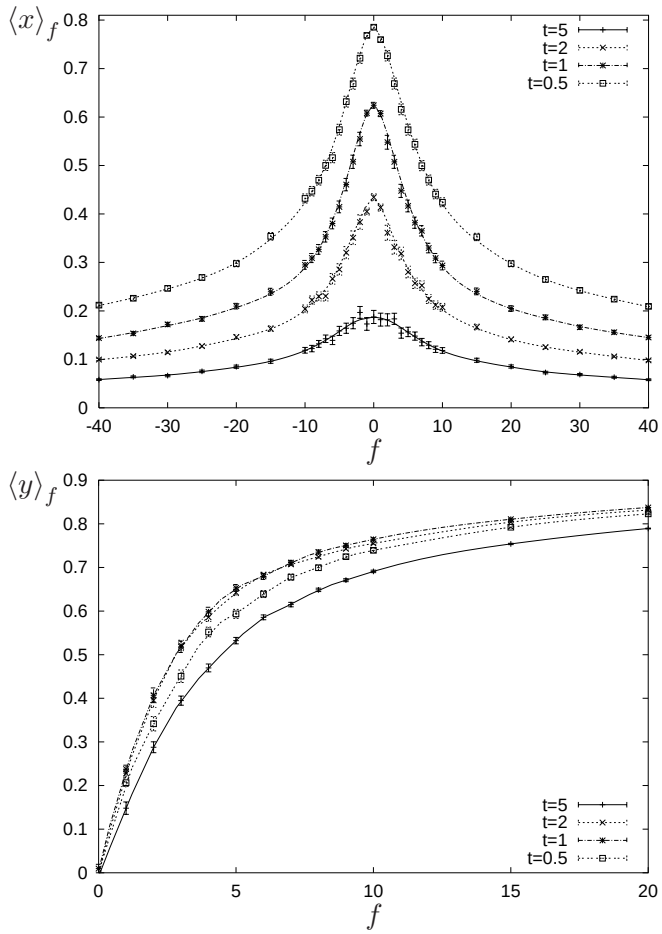


FIG. 3: Response to a transverse force, obtained by Monte Carlo simulations. Forces are measured in units of k_BT/L, lengths in units of L. Error bars are shown. (Above) Response in the clamping direction. (Below) Response in the transverse direction is odd with f: only part of the explored parameter region is shown for clarity.

The effects hereby reported are amenable to a direct comparison with experiments regarding cytoskeletal filaments, or even DNA. For instance, optical systems might be used to get the x or y projection of the radial distribution function for a particular class of semiflexible polymers. For F-Actin with $\ell_p \approx 16$ μm [6], the double peak effect should be well visible for a range of lengths, 12 μm $\lesssim L \lesssim$ 43 μm. In this parameter range the difference between the central relative minimum and the double peaks maxima results in 10% of the total length (see Fig. 1), in the range $1 \div 4$ μm that is well above the experimental precision of 0.05 μm reported by [6]. Hence F-Actin would provide an ideal benchmark for the effects we report. We emphasize that the double peak structure is a clear hallmark of semiflexibility and hence

it might be used to obtain a rough estimate of the persistence length of a particular polymer filament, as for instance the nanometer sized stalks of kinesins and myosins.

In summary, we have presented evidence from extensive Monte Carlo simulations that the parameter region corresponding to semiflexible polymers is hallmarked by the appearance of a series of effects in the radial distribution function and in the response of the clamped polymer to an external transverse force. A semiflexible polymer shows a distinct anisotropy in the probability distribution function of the free end along the direction of the clamped end. At intermediate stiffness, $L \approx \ell_p$, the distribution function shows a pronounced double peak structure in the transverse direction. Semiflexible polymers have been previously reported [11] to be anisotropic objects, i.e. to respond in different ways to forces applied in the clamping or transverse direction. Here we have shown that even their response to a force along the transverse direction alone is intrinsically anisotropic, being linear in the transverse direction and non-linear along the direction of the clamped end in the small force regime.

We acknowledge helpful discussions with P. Benetatos, A. Parmeggiani, J. Wilhelm, T. Franosch and K. Kroy. This research has been supported by a Marie Curie Fellowship under contract no. HPMF-CT-2001-01432.

[1] J. Howard, *Mechanics of Motor Proteins and the Cytoskeleton* (Sinauer Associates, Sunderland, 2001).

[2] A. Ott et al., Phys. Rev. E **48**, R1642 (1993).

[3] F. Gittes et al., J. Cell Biol. **120**, 923 (1993).

[4] J. Käs et al., Nature(London) **368**, 226 (1994).

[5] J. F. Marko and E. D. Siggia, Macromol. **28**, 8759 (1995).

[6] L. LeGoff et al., Phys. Rev. Lett. **89**, 258101 (2002).

[7] X. Liu and G. H. Pollack, Biophys. J. **83**, 2705 (2002).

[8] H. Yamakawa, *Modern Theory of Polymer Solutions* (Harper & Row, New York, 1971).

[9] L. D. Landau and E. M. Lifshitz, *Course of Theoretical Physics, Vol. 7* (Pergamon Press, London, 1959).

[10] J. Wilhelm and E. Frey, Phys. Rev. Lett. **77**, 2581 (1996).

[11] K. Kroy and E. Frey, Phys. Rev. Lett. **77**, 306 (1996).

[12] D. A. Head et al., cond–mat 0303499 (2003).

[13] J. Wilhelm and E. Frey, cond–mat 0303592 (2003).

[14] G. Lattanzi and E. Frey, unpublished.

[15] O. Kratky and G. Porod, Recl. Trav. Chim. **68**, 1106 (1949).

[16] N. Saitô et al., J. Phys. Soc. Japan **22**, 219 (1967).

[17] R. G. Winkler et al., J. Chem. Phys. **101**, 8119 (1994).

[18] T. Norisuye et al., Macromol. **11**, 966 (1978).

[19] F. MacKintosh et al., Phys. Rev. Lett. **75**, 4425 (1995).

[20] J. Wilhelm and E. Frey, unpublished.

[21] P. Benetatos and E. Frey, Phys. Rev. E **67**, 051108 (2003).

[22] C. Bracher, cond–mat 0304241 (2003).